Electronic Structure of Some Substituted Iron(II) Porphyrins. Are They Intermediate or High Spin?

Meng-Sheng Liao, John D. Watts, and Ming-Ju Huang*

Department of Chemistry, Jackson State University, P.O. Box 17910, Jackson, Mississippi 39217

Received: January 28, 2007; In Final Form: May 1, 2007

The electronic structure of some substituted, four-coordinate iron(II) porphyrins has been investigated with DFT methods. These systems include iron tetraphenylporphine (FeTPP), iron octamethyltetrabenzporphine (FeOTBP), iron tetra(α,α,α,α-orthopivalamide)phenylporphine (FeTpivPP, also called "picket fence" porphyrin), halogenated iron porphyrins ($FeTPPX_n$, X = F, Cl; $n = 20, 28$), and iron octaethylporphine (FeOEP). A number of density functionals were used in the calculations. Different from the popular, intermediate-spin FeTPP, the ground states of FeOTBP, $FeTPPCl_{28}$, and $FeTPPF_{20}\beta Cl_8$ are predicted to be high spin. The calculated result for FeOTBP is in agreement with the early experimental measurement, thereby changing the previous conclusion drawn from the calculations with only the BP functional (*J. Chem. Phys.* **2002**, *116*, 3635). But FeTpivPP might have an intermediate-spin ground state, a conclusion that is different from the "experimental" one. With a notably expanded Fe−N bond length, FeOEP might exist as an admixed-spin ($S = 1, 2$) state. We also calculated the electron affinities (EAs) for the various iron porphyrins and compared them to experiment. On the basis of the calculated trends in the EAs and in the orbital energies, the experimental EAs for FeTpivPP, $FeTPPF_{20}$, and $FeTPPCl_{28}$ may be too small by 0.4−0.5 eV.

1. Introduction

The electronic structure of the iron ion in iron porphyrin complexes has been the subject of much experimental and theoretical work because of its importance for understanding biological processes involving heme proteins.[1] For certain transition metals (e.g., Cr, Mn, Fe, Co), the open d-shells may result in a number of energetically close-lying electronic states. Ferrous (i.e., Fe^{II}) porphyrins, with six d-electrons, can exist as intermediate- ($S = 1$), low- ($S = 0$), and high-spin ($S = 2$) states, depending on the coordination and the environment of the iron ion. Many experimental studies have focused upon the electronic structures of iron tetraphenylporphine (FeTPP) and iron octaethylporphine (FeOEP), the two most popular synthetic iron porphyrins; they agree that the ground state is of intermediate spin, but differ in the details of the electronic configuration. A $^3A_{2g}$ ground state arising from the $(d_{xy})^2(d_\pi)^2(d_{z^2})^2$ configuration was indicated by Mössbauer,[2,3] magnetic,[4] and proton NMR[5,6] measurements on FeTPP. On the other hand, Raman spectra of FeOEP were interpreted in terms of a ^3E_g state arising from the $(d_{xy})^2(d_\pi)^3(d_{z^2})^1$ configuration.[7] A detailed analysis of the various experimental data by Sontum et al.[8] cast doubt on the assignment of the ground state of FeOEP as a ^3E_g state, which is also not supported by the calculations.[8]

There are two four-coordinate Fe^{II} porphyrin complexes which may be different from FeTPP or FeOEP: the so-called "picket-fence" porphyrin, iron tetra(α,α,α,α-orthopivalamide)-phenylporphine (FeTpivPP),[9−11] and iron octamethyltetrabenzporphine (FeOTBP).[12] Their magnetic moments were reported to be 5.0 μ_B and 5.9 μ_B, respectively, suggesting a high-spin ground state with $S = 2$. The specific reasons underlying this electronic ground state of Fe^{II} in FeTpivPP or FeOTBP would be of particular interest, since the ground state is intermediate spin in FeTPP or FeOEP.

With the existence of a number of low-lying states, the electronic structure of iron porphyrins has proven to be difficult to describe theoretically. The Hartree−Fock method is inadequate, as it does not account for electron correlation. Early HF calculations[13−15] on simple iron porphine (FeP) predicted a high-spin $^5A_{1g}$ state to be lower in energy than $^3A_{2g}$ by more than 1 eV. This failure was ascribed to the fact that the high-spin state is always favored in the HF-type theories since the HF exchange contains only Fermi correlation, but not Coulomb correlation.[16] In the same vein, recent high-quality CASPT2 studies[17,18] of FeP remain in disagreement with experiment since they predict the lowest state to be $^5A_{1g}$.

Naturally, density functional theory (DFT) has been applied to iron porphyrins and appears to be a good choice in this aspect. Calculations on FeP by Kozlowski et al.[19] using the BP and B3LYP functionals predicted the ground state to be $^3A_{2g}$, in agreement with the experiment on FeTPP. However, it is also known that the ability of DFT to calculate the relative spin-state energies is sensitive to the type of functionals.[19] We recently investigated the behaviors of a large variety of density functionals in describing the energetics for iron porphyrins and related compounds and found that several functionals, namely B3LYP, B97, B97-1, and τ-HCTH-hyb, were able to yield satisfactory results for all the systems considered.[20]

On the basis of our recent investigations,[20] we want to further explore the electronic structures of some substituted, four-coordinate iron porphyrins that include FeOTBP, FeTpivPP, $FeTPPF_{20}$, $FeTPPF_{28}$, $FeTPPCl_{28}$, and $FeTPPF_{20}\beta Cl_8$. The FeTPP and FeOEP systems were also included in the study for the sake of comparison.

FeOTBP was once calculated by one of us with the BP functional,[21] which gave an intermediate-spin ground state for this system. It is shown that BP greatly overestimates the energy

* Address correspondence to this author. E-mail: mhuang@chem.jsums.edu.

10.1021/jp070734z CCC: $37.00
Published on Web 06/09/2007

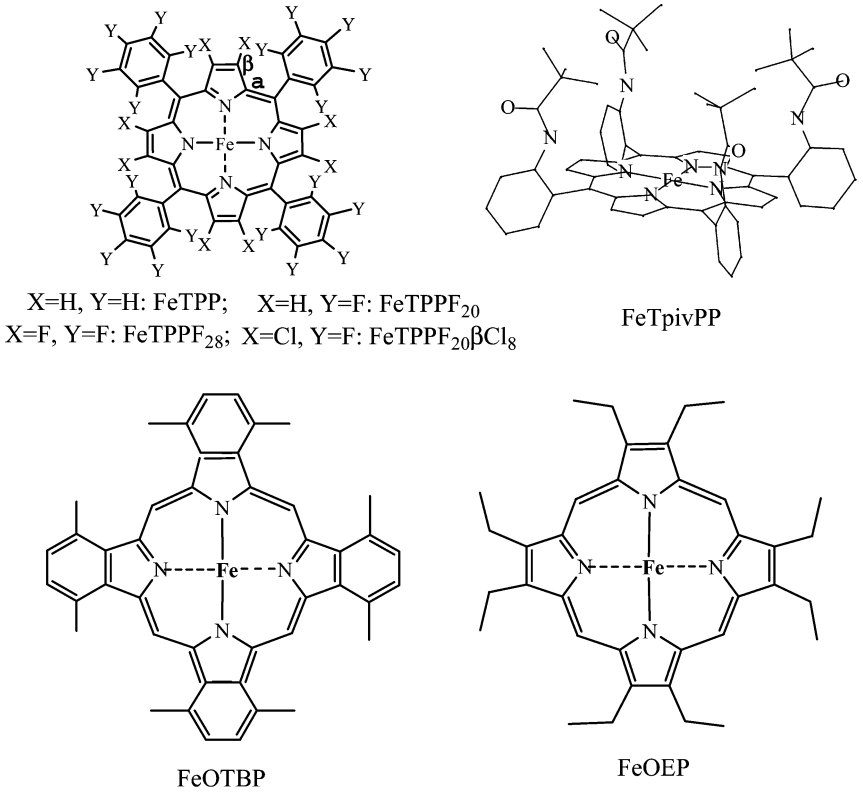

Figure 1. Molecular structures of the various iron porphyrins.

of the high-spin state, and so FeOTBP needs to be re-examined by using suitable functionals. FeTpivPP is the most studied heme model from an experimental point of view.[9] It has steric shielding on one side of the porphyrin, reversibly oxygenating in solution. This model simulates the stereochemical properties of myoglobin (Mb) and hemoglobin (Hb). Using the CPMD program, Rovira and Parrinello reported DFT/BP calculations on five-coordinate FeTpivPP(2-MeIm) and six-coordinate FeTpivPP(2-MeIm)(O_2) complexes,[22] but not on the unligated, four-coordinate one. Polyhalogenated metal porphyrins have attracted much interest because of their potential as selective oxidative catalysts. Chen et al.[23] measured the gas-phase electron affinities (EAs) of a series of substituted iron tetraphenylporphyrins including, among others, FeTpivPP, $FeTPPF_{20}$, $FeTPPCl_{28}$, and $FeTPPF_{20}\beta Cl_8$. In a recent study of $CoTPPF_{28}(L)_2$ (L is an axial ligand),[24] we showed that the F substituents at the β-pyrrole position cause a notable decrease in the relative energies of the high-spin states. On the basis of our recent results on FeP, we expect that some substituted, four-coordinate iron porphyrins may have a high-spin ground state. Traditionally, there was an argument[25] that an intermediate-spin Fe^{II} ion should be precisely centered among the four porphinato nitrogen atoms, whereas a high-spin Fe^{II} ion should lie substantially out of the porphyrin plane. The present investigations will help clarify the influence of the nature of the macrocycle on the electronic spin state of Fe^{II} in these systems.

2. Computational Details

The molecular structures of the various iron porphyrins studied here are illustrated in Figure 1. For computational convenience, taking a proper symmetry for the molecule is of importance. The macrocycle of porphyrins is conjugated and expected to be planar. Indeed, simple, unsubstituted transition metal porphines (MPs) exhibit a nearly planar D_{4h} structure.[26] But the larger MTPP appears to undergo a certain ruffling distortion in the crystal, depending upon the identity of the metal. For example, monoclinic ZnTPP belongs to the D_{4h} point group[27] while NiTPP adopts the classic S_4 ruffling.[28] It is logical to presume that these different structures are not too dissimilar in energy since, for example, H_2TPP crystallizes in both the triclinic form with an effectively planar macrocycle (D_{2h}) and the tetragonal form in which the macrocycle is distorted into C_{2v} symmetry.[29] Another example is NiOEP; it exists in three crystal forms: triclinic A and B are planar, whereas the tetragonal C form is ruffled.[30,31] In solution, NiTPP or NiOEP exists as a mixture of planar and ruffled conformers.[32−36] On the other hand, there have been some detailed theoretical investigations on the nonplanar distortion issue for H_2TPP,[37] NiP,[38] NiTPP,[36] and NiOEP.[39] It is found that the energy difference between a planar and a ruffled structure is very small for each system, consistent with the experimental observations mentioned above. Nickel porphyrins were particularly assumed to have a ruffling distortion as the ionic radius of Ni^{II} is relatively small (too small for the natural porphyrin cavity size). A ruffling of an iron porphyrin is expected to be smaller than that of a corresponding nickel porphyrin because the ionic radius of Fe^{II} (0.76 Å) is larger than that of Ni^{II} (0.72 Å). In fact, FeTPP possesses a quite planar framework in the crystalline phase.[2] Concerning the halogenated metal porphyrins $MTPPX_n$ (n = 20, 28), the substituents appear to produce little geometrical changes.[40] In the case of FeOTBP, there should be little or no S_4 ruffling of the porphyrin core because of the fused benzene rings in OTBP.[12]

On the basis of the above discussion, we have taken a high symmetry for each of the systems in the calculations. That is, $FeTPPX_n$ (n = 0, 20, 28) and FeOTBP were assumed to belong to the D_{4h} point group, whereas C_{4v} symmetry was adopted for FeTpivPP. The four phenyl groups of TPP were assumed to be

TABLE 1: Functionals Used in the Calculations

functional	formulation
BP	Becke's 1988 gradient correction for exchange (ref 45) plus Perdew's 1986 gradient correction for correlation (ref 46)
PBE	Perdew−Burke−Ernzerhof's 1996 corrections for both exchange and correlation (ref 47)
revPBE	revised PBE functional proposed in 1998 by Zhang and Yang (ref 48)
RPBE	revised PBE functional proposed in 1999 by Hammer, Hansen, and Nørskov (ref 49)
mPBE	modified PBE functional proposed in 2002 by Adamo and Barone (ref 50)
BOP	Becke's 1988 correction for exchange plus Tsuneda−Suzumura−Hirao's 1999 one-parameter progressive correlation functional (ref 51)
OPBE	Handy−Cohen's 2001 OPTX correction for exchange (ref 52) plus Perdew−Burke−Ernzerhof's 1996 correction for correlation
OPerdew	OPTX correction for exchange plus Perdew's 1986 gradient correction for correlation
OLYP	OPTX correction for exchange plus LYP correlation functional (ref 53)
HCTH/407	Hamprecht−Cohen−Tozer−Handy 1998 correction for both exchange and correlation (ref 54), containing 15 parameters refined against data from a training set of 407 atomic and molecular systems (ref 55)
Becke00	Becke's 2000 correction for both exchange and correlation, where the kinetic-energy density τ [$=\sum(\nabla\phi_i)^2$] is included (ref 56)
τ-HCTH	the kinetic-energy density τ is included in the HCTH/407 form (ref 57)
B3LYP	Becke's 1993 three-parameter hybrid functional (ref 58), using the LYP correlation functional
B97	Becke's 1997 hybrid functional that contains 10 adjustable parameters (ref 59)
B97−1	the adjustable parameters in B97 were reoptimized in a self-consistent manner (ref 54)
τ-HCTH-hyb	HF exchange is introduced into the τ-HCTH functional (ref 57)

perpendicular to the porphyrin plane, as shown by experiments.[2,40] Distorted conformers, if any, were not considered here.

All calculations were carried out with the Amsterdam Density Functional (ADF) program package (version 2005.01).[41−44] To obtain reliable results and for the sake of comparison, a number of density functionals[45−59] were used in the calculations; they include GGA functionals (BP, PBE, RPBE, revPBE, mPBE, BOP, OPBE, OPerdew, OLYP, HCTH/407) that contain a generalized gradient approximation (GGA) correction, meta-GGA functionals (Becke00, τ-HCTH) that contain the electron kinetic energy density τ [$=\sum(\nabla\phi_i)^2$] (in addition to GGA), and hybrid-GGA functionals (B3LYP, τ-HCTH-hyb, B97, B97-1) that contain a fraction of the HF (or exact) exchange. A brief description of their formulation is given in Table 1. The various functionals have their specific advantages and disadvantages. For example, BP and PBE yield reliable results for the intermediate-spin states but overestimate the energies of the high-spin states. The OPBE, OPerdew, and OYLP functionals that use the OPTX correction for exchange show good performance for calculating the high-spin energetics of some iron porphyrins,[60,61] but their results for the intermediate-spin states are questionable.[20] The hybrid-GGA functionals considered here are able to provide a reliable description of different electronic states of iron porphyrins,[20] but calculations with them are very time-consuming within the ADF framework when the calculated systems are large. In many cases, meta-GGAs perform comparably to the hybrid-GGA, and τ was thought to be a good alternative to the HF exchange mixing.[56] It would be of interest to compare the performances of the DFT methods for calculations on these iron porphyrins.

In the present version of ADF, the meta-GGA and hybrid-GGA functionals are treated in a non-self-consistent field (non-SCF) manner. That is, the meta-GGA or hybrid-GGA energies are evaluated with orbitals and densities from LDA or GGA calculations. Previous calculations by us[24] and others[49] show that non-SCF and SCF procedures yield very close results. Because these functionals do not have an implementation for the exchange-correlation (XC) potential, geometry optimizations cannot be performed with them. In our calculations, the molecular structures are optimized by using the BP functional. Generally, DFT (e.g., the BP functional) gives an excellent description of the molecular structure of a given electronic state for transition metal systems.[62] The changes in calculated molecular structure with use of different functionals are in fact small and do not lead to notable errors in the calculated energies.[24] To further support these arguments, Supporting Information has been provided, which presents (1) the optimized Fe−N bond lengths for selected states of FeTPP and FeOTBP with different functionals and (2) a comparison between the non-SCF and SCF calculated relative energies for selected states of FeTPP and FeOTBP with the PBE, OPBE, or OLYP functional. For any molecule in any state, R_{Fe-N} changes by less than 0.02 Å from one functional to another, although two different functionals (e.g., BP and OPBE) can give rather different relative energies for a state. On the other hand, the non-SCF calculated relative energies are indeed very close to the SCF ones with any functional used here, consistent with previous calculations.[24,49]

The STO basis set employed is the standard ADF-TZP set, which is triple-ζ for valence orbitals plus one polarization function. To obtain accurate results, the valence set on Fe included subvalence 3s and 3p shells. For C, N, F, and O, 2s and 2p were included as valence shells. The other shells of lower energy, i.e., [Ne] for Fe and [He] for C/N/F/O, were treated as core and kept frozen according to the frozen-core approximation.[41] Relativistic corrections for the valence electrons were calculated by the quasirelativistic (QR) method.[63] For the open-shell states, the unrestricted Kohn−Sham (KS) spin-density functional approach was adopted. Spin contamination in the unrestricted calculations was found to be small, as is shown in other calculations on comparable compounds.[16,60,61] Hence, the energetics obtained from the DFT calculations can be expected to be meaningful.

3. Results and Discussion

Placing the molecule in the *xy* plane, the five metal 3d-orbitals transform as, in D_{4h} symmetry, a_{1g} (d_{z^2}), b_{1g} ($d_{x^2-y^2}$), e_g (d_π, i.e., d_{xz} and d_{yz}), and b_{2g} (d_{xy}). Different occupations of six electrons in these d-orbitals can yield a number of possible low-lying states. To determine the ground state, relative energies of eight selected configurations were calculated; they include four intermediate-spin ($S = 1$), three high-spin ($S = 2$), and one low-spin ($S = 0$) states. Geometry optimization was performed (using the BP functional) separately for each state considered. It should be pointed out again that the structures of the various states can be well described by different density functionals.

TABLE 2: Optimized Equatorial Fe−N Bond Lengths (*R*, in Å) for Selected States of the Various Iron Porphyrins with the BP Functional

configuration					R_{Fe-N}						
d_{xy}	d_{z^2}	d_π	$d_{x^2-y^2}$	state	FeTPP	FeOTBP	$FeTPPF_{28}$	$FeTPPCl_{28}$	$FeTPPF_{20}$	$FeTPPF_{20}\beta Cl_8$	FeOEP
2	2	2	0	$^3A_{2g}$	1.965	2.005	1.982	1.998	1.966	1.998	1.996
2	1	3	0	^3E_g (A)	1.967	2.011	1.985	2.000		2.001	1.999
1	1	4	0	$^3B_{2g}$	1.975	2.016	2.000	2.010			
1	2	3	0	^3E_g (B)	1.966	2.007	1.984	1.999			
1	2	2	1	$^5A_{1g}$	2.031	2.074	2.054	2.059	2.032	2.061	2.057
1	1	3	1	^5E_g	2.037	2.077	2.063	2.066			
2	1	2	1	$^5B_{2g}$	2.029	2.072	2.047	2.046			
2	0	4	0	$^1A_{1g}$	1.981	2.023	2.003	2.015			
experimental bond length					1.972						

TABLE 3: Optimized Structural Parameters (distance *R*, in Å)[a] for Selected States of FeTpivPP with the BP Functional

configuration								
d_{xy}	d_{z^2}	d_π	$d_{x^2-y^2}$	state	R_{Fe-N}	$R_{Ct(N4)\cdots Fe}$	$R_{Ct(N4)\cdots Ct(C8)}$	$R_{Ct(N4)\cdots Ct(H8)}$
2	2	2	0	$^3A_2$	1.967	0.012	0.081	0.169
2	1	3	0	^3E (A)	1.970	0.010	0.080	0.168
1	1	4	0	$^3B_2$	1.980	0.010	0.086	0.176
1	2	3	0	^3E (B)	1.969	0.013	0.081	0.169
1	2	2	1	$^5A_1$	2.035	0.020	0.110	0.222
1	1	3	1	^5E	2.041	−0.015[b]	0.100	0.202
2	1	2	1	$^5B_2$	2.033	−0.016	0.102	0.204
2	0	4	0	$^1A_1$	1.986	−0.057	0.085	0.173

[a] Ct(N4): centroid of the plane defined by the four pyrrole nitrogen atoms. Ct(C8): centroid of the plane defined by the eight peripheral carbon atoms. Ct(H8): centroid of the plane defined by the eight peripheral hydrogen atoms. [b] Negative value for $R_{Ct(N4)\cdots Fe}$ means that Fe displaces out of the porphyrin plane toward the unencumbered side of the porphyrin.

For the considered ^3E_g(A), ^3E_g(B), and ^5E_g states, three electrons occupy the degenerate e_g/d_π orbitals. According to the Jahn−Teller theorem, the molecule will be unstable and will undergo a geometrical distortion that removes the degeneracy. In our case, the symmetry of the molecule will be lowered to D_{2h}. We have investigated the spontaneous Jahn−Teller effect for these states in FeTPP. In reduced D_{2h} symmetry, the e_g/d_π orbitals are split into b_{2g}/d_{xz} and b_{3g}/d_{yz}. Geometry optimizations were carried out under D_{2h} symmetry and with a $(b_{3g}/d_{yz})^2(b_{2g}/d_{xz})^1$ occupation. The calculated relative energies and Fe−N bond lengths for selected states of FeTPP in D_{4h} and D_{2h} symmetries are also provided in the Supporting Information (Table S3) together with a figure (Figure S1) that displays the orbital energy level diagrams of FeTPP in the ^3E_g(A) (D_{4h}) and $^3B_{2g}$ (D_{2h}) states. When the constraints of D_{4h} symmetry are relaxed to D_{2h}, the Fe−N1 distance becomes 0.01−0.02 Å shorter than Fe−N2. The smallness of this distortion may be attributed to the rigidity of the porphyrin macrocycle. The total molecular energy is lowered by 0.07−0.08 eV. This energetic stabilization is not large enough to change the ground state ($^3A_{2g}$) obtained by a number of GGA functionals. Consequently, we neglected Jahn−Teller effects for all the excited ^3E_g(A), ^3E_g(B), and ^5E_g states.

The optimized equatorial Fe−N bond lengths (R_{Fe-N}) for the molecules with D_{4h} symmetry are collected in Table 2, together with available experimental data for FeTPP in the crystal.[2] (No out-of-plane displacement of Fe has been found in any of the electronic states. See also ref 21.) Table 3 reports the optimized structural parameters for FeTpivPP; they include R_{Fe-N}, $R_{Ct(N4)\cdots Fe}$ (the displacement of the metal out of the porphyrin plane), and $R_{Ct(N4)\cdots Ct(C8)}$ or $R_{Ct(N4)\cdots Ct(H8)}$ (a measure of the doming of the macrocycle ring).

3.1. FeTPP. The calculated relative energies ($E^{relative}$) for selected states of FeTPP with various density functionals are presented in Table 4 (the $E^{relative}$ of $^3A_{2g}$ is set to zero). Compared to the previous results on the simple FeP,[20] the $E^{relative}$ values for FeTPP have little changes. The main results here can be summarized as follows: (1) With the BP functional, the calculated ground state is $^3A_{2g}$, in agreement with most of the experiments;[2−6] $^5A_{1g}$ is the lowest quintet state, lying 0.73 eV above the ground state. (2) The PBE and BOP functionals yield results which are similar to those of BP, while a revised or modified PBE (i.e., RPBE, revPBE, or mPBE) leads to a decrease in the relative energies of the high-spin states (by 0.1−0.2 eV for $^5A_{1g}$). (3) The functionals that use the OPTX exchange yield very different results from those of the other GGA functionals. First, OPBE, OPerdew, and OLYP predict the ^3E_g(A) state to be lower than $^3A_{2g}$ in energy, in contrast to the energy ordering obtained by the other GGA functionals. In addition, the high-spin states now have rather small relative energies (0.25−0.30 eV for $^5A_{1g}$). (4) With the HCTH/407 functional, the relative energies of the high-spin states become even smaller (only 0.04 eV for $^5A_{1g}$). (5) By including the kinetic energy density τ in the HCTH functional, the relative energies of the high-spin states are further decreased. Now, $^5A_{1g}$ has become the ground state and lies 0.17 eV below the $^3A_{2g}$ state. But this is qualitatively inconsistent with experiment. (6) With the hybrid-GGA functionals, the $^5A_{1g}-^3A_{2g}$ energy gap is estimated to be 0.1−0.2 eV, which is believed to be a reliable energy range based on a recent study.[20] (Not all spin states were calculated by using the hybrid-GGA functionals because calculations of large systems with them are very time-consuming within the ADF framework.)

3.2. FeOTBP. The results for FeOTBP are presented in Table 5. With the BP functional, the intermediate-spin state $^3A_{2g}$ is calculated to be the lowest in energy, similar to the situation for FeTPP. But the results indicate a significant decrease in the relative energies of the high-spin states from FeTPP to FeOTBP. Here the BP value of $E^{relative}$ for $^5A_{1g}$ is only 0.48 eV. On the basis of the recent study[20] and the results for FeTPP, the BP functional overestimates the relative energy of the high-spin state by 0.5−0.6 eV. Therefore, the $^5A_{1g}$ state in FeOTBP is expected to be lower than $^3A_{2g}$ in energy. This expectation is confirmed by the calculations with the OPBE, OPerdew, OLYP, and the

TABLE 4: Calculated Relative Energies (*E*, eV) for Selected States of FeTPP with Various Density Functionals

		$E^{relative}$, eV							
		$^3A_{2g}$	$^3E_g(A)$	$^3B_{2g}$	$^3E_g(B)$	$^5A_{1g}$	^5E_g	$^5B_{2g}$	$^1A_{1g}$
GGA	BP	0	0.12	0.26	0.70	0.73	0.86	1.08	1.49
	PBE	0	0.11	0.25	0.67	0.70	0.82	1.06	1.47
	RPBE	0	0.11	0.23	0.68	0.53	0.66	0.90	1.43
	revPBE	0	0.10	0.22	0.68	0.57	0.69	0.93	1.43
	mPBE	0	0.11	0.25	0.68	0.66	0.78	1.02	1.47
	BOP	0	0.17	0.32	0.73	0.71	0.86	1.13	1.33
	OPBE	0	−0.11	0.05	0.56	0.26	0.27	0.49	1.38
	OPerdew	0	−0.07	0.09	0.57	0.27	0.31	0.53	1.44
	OLYP	0	0.00	0.16	0.61	0.29	0.37	0.65	1.39
	HCTH/407	0	0.04	0.19	0.54	0.04	0.17	0.49	1.56
meta-GGA	Becke00	0	0.10	0.23	0.62	0.33	0.43	0.79	1.35
	τ-HCTH	0	0.06	0.29	0.56	−0.17	−0.01	0.30	1.65
Hybrid-GGA	B3LYP	0				0.19			
	τ-HCTH-hyb	0				0.16			
	B97	0				0.12			
	B97-1	0				0.12			

TABLE 5: Calculated Relative Energies (*E*, eV) for Selected States of FeOTBP with Various Density Functionals

		$E^{relative}$, eV							
		$^3A_{2g}$	$^3E_g(A)$	$^3B_{2g}$	$^3E_g(B)$	$^5A_{1g}$	^5E_g	$^5B_{2g}$	$^1A_{1g}$
GGA	BP	0	0.12	0.20	0.75	0.48	0.61	0.83	1.43
	PBE	0	0.11	0.18	0.72	0.45	0.57	0.81	1.42
	RPBE	0	0.11	0.15	0.73	0.25	0.40	0.63	1.37
	revPBE	0	0.10	0.15	0.73	0.29	0.43	0.66	1.37
	mPBE	0	0.11	0.18	0.72	0.39	0.52	0.77	1.41
	BOP	0	0.15	0.24	0.77	0.44	0.59	0.88	1.25
	OPBE	0	−0.09	0.01	0.62	−0.06	−0.02	0.20	1.35
	OPerdew	0	−0.06	0.05	0.63	−0.04	0.02	0.24	1.41
	OLYP	0	0.01	0.12	0.67	−0.02	0.09	0.36	1.35
	HCTH/407	0	0.04	0.16	0.59	−0.25	−0.10	0.23	1.52
meta-GGA	Becke00	0	0.13	0.29	0.69	0.16	0.30	0.63	1.41
	τ-HCTH	0	0.08	0.22	0.62	−0.49	−0.30	−0.01	1.59
Hybrid-GGA	B3LYP	0				−0.03			
	τ-HCTH-hyb	0				−0.05			
	B97	0				−0.10			
	B97-1	0				−0.08			

TABLE 6: Calculated Relative Energies (*E*, eV) for Selected States of FeTpivPP with Various Density Functionals

		$E^{relative}$, eV							
		$^3A_2$	$^3E(A)$	$^3B_2$	$^3E(B)$	$^5A_1$	^5E	$^5B_2$	$^1A_1$
GGA	BP	0	0.13	0.27	0.70	0.73	0.86	1.08	1.49
	PBE	0	0.10	0.20	0.69	0.64	0.77	1.01	1.37
	RPBE	0	0.11	0.17	0.70	0.48	0.61	0.85	1.34
	revPBE	0	0.13	0.17	0.70	0.52	0.64	0.87	1.33
	mPBE	0	0.11	0.20	0.69	0.60	0.73	0.97	1.36
	BOP	0	0.16	0.26	0.75	0.66	0.81	1.08	1.23
	OPBE	0	−0.12	0.01	0.57	0.20	0.21	0.44	1.30
	OPerdew	0	−0.09	0.04	0.59	0.21	0.26	0.48	1.35
	OLYP	0	−0.01	0.12	0.63	0.24	0.32	0.60	1.30
	HCTH/407	0	0.04	0.15	0.56	−0.02	0.13	0.45	1.45
meta-GGA	Becke00	0	0.10		0.63	0.28	0.36	0.71	1.28
	τ-HCTH	0	0.06		0.58	−0.20	−0.03	0.28	1.54
Hybrid-GGA	B3LYP	0				0.15			
	τ-HCTH-hyb	0				0.10			
	B97	0				0.05			
	B97-1	0				0.06			

hybrid-GGA functionals; their $E^{relative}$ values for $^5A_{1g}$ are all negative here, indicating that FeOTBP is high spin. This is in contrast to the previous conclusion drawn from the BP results only.[21] According to Table 2, the Fe−N bond in FeOTBP is notably longer (by ∼0.04) than that in FeTPP. This lengthening of the bond changes the spin state.

3.3. FeTpivPP. The results for FeTpivPP are presented in Table 6. In contrast to FeOTBP, the ground state of FeTpivPP is predicted to be $^3A_{2g}$, i.e., the same as that of FeTPP. Even the BP calculated $E^{relative}$ of $^5A_{1g}$ in FeTpivPP is the same as that for FeTPP. But the calculations with the other functionals show a decrease in the $^5A_{1g}$ relative energy by 0.04−0.07 eV from FeTPP to FeTpivPP. This energy decrease seems to be too small to cause the ground state to change from the intermediate- to the high-spin state because, according to the "reliable" calculations with the hybrid-GGA functionals, $^5A_{1g}$ in FeTpivPP still lies 0.05−0.15 eV above $^3A_{2g}$. We note that the calculation with HCTH yields a slightly negative $E^{relative}$ for $^5A_{1g}$ in FeTpivPP and also suggests that FeTPP is intermediate spin. The trend in the HCTH results seems to be qualitatively consistent with the argument[64] that FeTpivPP is different from FeTPP in spin state. However, the HCTH functional probably

TABLE 7: Calculated Relative Energies (*E*, eV) for Selected States of $FeTPPF_{28}$ with Various Density Functionals

		$E^{relative}$, eV							
		$^3A_{2g}$	$^3E_g(A)$	$^3B_{2g}$	$^3E_g(B)$	$^5A_{1g}$	^5E_g	$^5B_{2g}$	$^1A_{1g}$
GGA	BP	0	0.10	0.35	0.82	0.64	0.74	0.90	1.49
	PBE	0	0.09	0.33	0.79	0.74	0.85	0.99	1.49
	RPBE	0	0.09	0.29	0.80	0.53	0.66	0.80	1.44
	revPBE	0	0.08	0.29	0.80	0.58	0.69	0.83	1.44
	mPBE	0	0.09	0.32	0.79	0.68	0.80	0.94	1.48
	BOP	0	0.13	0.36	0.84	0.71	0.84	1.03	1.31
	OPBE	0	−0.11	0.17	0.68	0.25	0.28	0.41	1.45
	OPerdew	0	−0.08	0.20	0.69	0.28	0.33	0.46	1.51
	OLYP	0	−0.01	0.25	0.73	0.29	0.37	0.56	1.43
	HCTH/407	0	0.02	0.27	0.65	0.04	0.17	0.43	1.59
meta-GGA	Becke00	0	0.16	0.49	0.78	0.56	0.69	0.98	1.58
	τ-HCTH	0	0.04	0.34	0.68	−0.19	−0.03	0.14	1.65
Hybrid-GGA	B3LYP	0				0.21			
	τ-HCTH-hyb	0				0.20			
	B97	0				0.13			
	B97-1	0				0.15			

TABLE 8: Calculated Relative Energies (*E*, eV) for Selected States of $FeTPPCl_{28}$ with Various Density Functionals

		$E^{relative}$, eV							
		$^3A_{2g}$	$^3E_g(A)$	$^3B_{2g}$	$^3E_g(B)$	$^5A_{1g}$	^5E_g	$^5B_{2g}$	$^1A_{1g}$
GGA	BP	0	0.10	0.33	0.81	0.45	0.55	0.72	1.48
	PBE	0	0.08	0.31	0.78	0.42	0.52	0.70	1.46
	RPBE	0	0.10	0.29	0.81	0.24	0.35	0.54	1.42
	revPBE	0	0.10	0.28	0.80	0.28	0.38	0.56	1.42
	mPBE	0	0.09	0.30	0.79	0.37	0.47	0.66	1.45
	BOP	0	0.14	0.36	0.85	0.40	0.52	0.74	1.28
	OPBE	0	−0.12	0.13	0.66	−0.06	−0.03	0.14	1.40
	OPerdew	0	−0.09	0.16	0.68	−0.04	0.01	0.17	1.46
	OLYP	0	−0.02	0.22	0.72	−0.03	0.05	0.27	1.39
	HCTH/407	0	0.01	0.24	0.63	−0.28	−0.16	0.14	1.54
meta-GGA	Becke00	0	0.08	0.33	0.73	0.06	0.18	0.59	1.38
	τ-HCTH	0	0.07	0.36	0.70	−0.47	−0.31	−0.09	1.65
Hybrid-GGA	B3LYP	0				−0.08			
	τ-HCTH-hyb	0				−0.09			
	B97	0				−0.14			
	B97-1	0				−0.12			

TABLE 9: Calculated Relative Energies (*E*, eV) for Selected States of $FeTPPF_{20}$, $FeTPPF_{20}\beta Cl_8$, and FeOEP with Various Density Functionals

		$E^{relative}$, eV							
		$FeTPPF_{20}$		$FeTPPF_{20}\beta Cl_8$			FeOEP		
		$^3A_{2g}$	$^5A_{1g}$	$^3A_{2g}$	$^3E_g(A)$	$^5A_{1g}$	$^3A_{2g}$	$^3E_g(A)$	$^5A_{1g}$
GGA	BP	0	0.73	0	0.09	0.45	0	0.18	0.57
	PBE	0	0.72	0	0.14	0.45	0	0.17	0.54
	RPBE	0	0.58	0	0.15	0.27	0	0.17	0.38
	revPBE	0	0.62	0	0.14	0.31	0	0.16	0.41
	mPBE	0	0.68	0	0.14	0.40	0	0.17	0.50
	BOP	0	0.77	0	0.19	0.45	0	0.21	0.56
	OPBE	0	0.23	0	−0.06	−0.04	0	−0.05	0.07
	OPerdew	0	0.25	0	−0.03	−0.02	0	−0.02	0.09
	OLYP	0	0.30	0	0.04	0.01	0	0.06	0.12
	HCTH/407	0	0.01	0	0.06	−0.25	0	0.10	−0.13
meta-GGA	Becke00	0	0.43	0	0.17	0.15	0	0.16	0.24
	τ-HCTH	0	−0.10	0	0.12	−0.44	0	0.13	−0.35
Hybrid-GGA	B3LYP	0	0.19	0		−0.05	0		0.06
	τ-HCTH-hyb	0	0.17	0		−0.10	0		0.01
	B97	0	0.12	0		−0.13	0		−0.02
	B97-1	0	0.12	0		−0.12	0		−0.01

underestimates the relative energies of the high-spin states.[20] Examining the calculated structural parameters of FeTpivPP (Table 3), we see that the equatorial Fe−N bond length in this complex shows very slight core expansion (<0.01 Å) as compared to that in FeTPP. The displacement of Fe from the porphyrin plane is very small even in the high-spin state (0.02 Å), as is the doming of the macrocycle ring. It seems that the bulky substituents at the *meso*-phenyl positions have a rather limited influence on the electronic state of the iron porphyrin.

3.4. $FeTPPF_{28}$ and $FeTPPCl_{28}$. The results for these two systems are presented in Tables 7 and 8 , respectively. For a given state, the Fe−N bond length in $FeTPPF_{28}$ is about 0.02 Å larger than that in FeTPP. As a result, the $E^{relative}$ of $^5A_{1g}$ is 0.1 eV lower for the former than for the latter system according to the BP results. However, the other functionals do

not yield a decrease in the high-spin state's relative energy from FeTPP to $FeTPPF_{28}$, indicating that this halogenated system has the same $^3A_{2g}$ ground state as FeTPP.

In the case of $FeTPPCl_{28}$, the calculated Fe−N bond length of a given state is about 0.01 Å smaller than that in FeOTBP but 0.02 Å larger than that in $FeTPPF_{28}$. Contrary to the fluoride, the chloride system is predicted to be high spin, and most functionals predict the $E^{relative}$ of $^5A_{1g}$ to be even slightly lower than that in FeOTBP.

3.5. $FeTPPF_{20}$, $FeTPPF_{20}\beta Cl_8$, and FeOEP. The results for these three systems are collected in Table 9. Here only the states of particular interest were calculated. An $FeTPPF_{20}$ system was also considered because we want to see how the Cl substituents at the β positions influence the electronic structure of the iron porphyrin. According to the calculations, the Fe−N bond length for any given state in $FeTPPF_{20}$ is very close to that in FeTPP, indicating that the F substituents at the *meso*-phenyl positions have little effect on the molecular structure of the iron porphyrin. For $^5A_{1g}$ in $FeTPPF_{20}$, most GGA and all hybrid-GGA functionals yield an $E^{relative}$ that is the same or nearly the same as that in FeTPP. These results indicate that $FeTPPF_{20}$ is not different from FeTPP for both R_{Fe-N} and $E^{relative}$.

From $FeTPPF_{20}$ to $FeTPPF_{20}\beta Cl_8$, the Fe−N bond lengthens and the relative energy of the high-spin state is lowered significantly. $FeTPPF_{20}\beta Cl_8$ is actually very similar to $FeTPPCl_{28}$ for both R_{Fe-N} and $E^{relative}$, and so it should also be a high-spin system.

Concerning FeOEP, the Fe−N bond length calculated for a given state is nearly the same as that in $FeTPPF_{20}\beta Cl_8$, the difference in R_{Fe-N} between the two systems being less than 0.005 Å. Being electron-donating substituents, the ethyl groups seem to cause a smaller decrease in the high-spin state's relative energy than do the Cl substituents; the $E^{relative}$ of $^5A_{1g}$ in FeOEP is systematically ∼0.1 eV higher than that in $FeTPPF_{20}\beta Cl_8$, independent of the functional used. Thus, the B3LYP functional, which yields a negative $E^{relative}$ of −0.05 eV for $^5A_{1g}$ in $FeTPPF_{20}\beta Cl_8$, gives a positive value of 0.06 eV for $^5A_{1g}$ in FeOEP. Then, the calculations with the other hybrid-GGA functionals show $^3A_{2g}$ and $^5A_{1g}$ to be nearly degenerate, the energy difference being at most 0.02 eV between the two states. FeOEP was suggested to be intermediate spin in the literature.[64] The room temperature susceptibility of the system indicated an effective magnetic moment of 4.7 μ_B, which lies between the spin-only values of 2.8 and 4.9 μ_B expected for $S = 1$ and 2 states, respectively, but larger than the value 4.4 μ_B measured for FeTPP.[2] On the basis of calculation and experiment, we hypothesize that FeOEP might exist as an admixed-spin ($S = 1$, 2) state.

The orbital energy level diagrams of the various iron porphyrins are illustrated in Figure 2. The orbital energy levels are shifted down from FeTPP to FeTpivPP to $FeTPPF_{20}$ to $FeTPPF_{20}\beta Cl_8$ and then shifted up from $FeTPPF_{20}\beta Cl_8$ to $FeTPPCl_{28}$. The antibonding b_{1g} orbital ($d_{x^2-y^2}$) is particularly destabilized through its interaction with the porphyrin nitrogens so that it lies above the porphyrin antibonding b_{1u} orbital in FeTPP. FeTpivPP is different from FeTPP in that b_{1g} lies below b_{1u} in the former. In this respect, FeTpivPP is similar to $FeTPPF_{20}\beta Cl_8$ or $FeTPPCl_{28}$; the latter two systems are predicted to be high spin. If we compare the energy level diagram of FeOTBP to that of FeTPP, we can see that the addition of four benzo groups to the porphyrin ring removes the near degeneracy of a_{2u} and a_{1u}, raising the latter to a large extent. Owing to a lengthening of the Fe−N bond in FeOTBP, the b_{1g} ($d_{x^2-y^2}$) orbital is lowered and so it becomes occupied in this system.

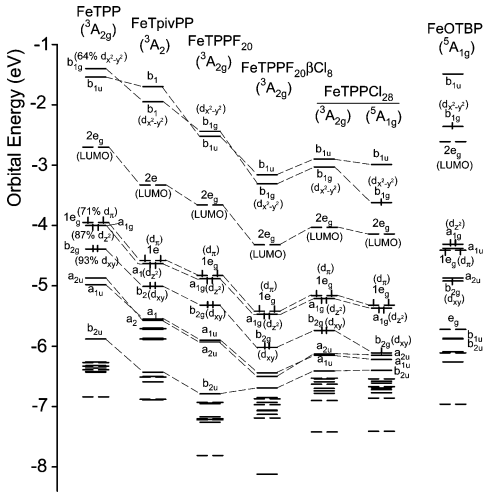

Figure 2. Orbital energy levels of the various iron porphyrins.

3.6. Electron Affinities. There have been experimental measurements of electron affinities (EAs) for a series of substituted iron porphyrins in the gas phase.[23] The EA of a halogenated metal porphyrin is suggested to be a useful measure of electronic effects on catalyst activity.[23] We have thus calculated EAs for most systems studied here. It would be of interest to make comparison between the experimental and calculated EAs. Another purpose of these calculations is to examine whether the EAs are significantly different for different spin states. To better examine the accuracy of the density functionals in predicting the EAs, we included in the calculations another two systems, namely FeTPP(Cl) (Cl is an axial ligand here) and NiTPP, for which experimental gas-phase EAs are available as well.[23]

The calculated EAs for the various iron porphyrins and NiTPP with various functionals are collected in Table 10. They were obtained by the so-called ΔSCF method in which separate SCF calculations for the neutral molecule and its anion are carried out and $-EA = E(X^-) - E(X)$. One obvious feature of the EA values is that the calculated EAs for the intermediate- and high-spin states are very close for every system with any functional. Another feature here is that the added electron in the iron porphyrin always goes into the $1e_g$ (d_π) orbital, whether the system is in an intermediate- or high-spin state. This may be the reason why the different spin states have close EAs. In this case, the calculated EAs for different spin states cannot be used to judge whether an iron porphyrin is intermediate spin or high spin.

Examining the BP results, we see that the calculated EAs for FeTPP, $FeTPPF_{20}\beta Cl_8$, $FeTPP_{28}$, FeTPP(Cl), and NiTPP agree very well with the experimental values, the error being less than 0.1 eV. The HCTH/407 results are the same or nearly the same as the BP ones (for every system). The other functionals give EAs which are more or less smaller than those obtained with BP; in fact, the calculated EAs are not very sensitive to the functional used. For FeTpivPP, $FeTPPCl_{28}$, and $FeTPPF_{20}$, however, the EAs of BP are too large by about 0.5 eV as compared to the experimental data. According to the calculation, the EA increases by ca. 0.2 eV from $FeTPPCl_{28}$ to $FeTPPF_{20}\beta Cl_8$. But from the experiment, the magnitude of this increase is as large as 0.6 eV. It is shown that the lower the orbital energy levels are (see Figure 2), the larger the EAs. Moreover, the magnitude of the increase of the calculated EA from one system to another is found to be consistent with the magnitude of the decrease of the $1e_g$ orbital energy. To facilitate comparison among these quantities, Figure 3 displays the

TABLE 10: Calculated Electron Affinities (EA, in eV) for Various Iron Porphyrins and NiTPP

	EA, eV												
	FeTPP		FeTpivPP		$FeTPPCl_{28}$		$FeTPPF_{20}$	$FeTPPF_{20}\beta Cl_8$		$FeTPPF_{28}$	FeTPP(Cl)[a]		NiTPP
	$^3A_{2g}$	$^5A_{1g}$	$^3A_2$	$^5A_1$	$^3A_{2g}$	$^5A_{1g}$	$^3A_{2g}$	$^3A_{2g}$	$^5A_{1g}$	$^3A_{2g}$	$^4A_2$	$^6A_1$	$^1A_{1g}$
BP	1.82	1.83	2.51	2.53	3.09	3.12	2.63	3.30	3.32	3.17	2.10	2.13	1.48
PBE	1.74	1.75	2.44	2.45	3.00	3.03	2.55	3.21	3.23	3.08	2.02	2.04	1.40
RPBE	1.64	1.65	2.32	2.34	2.89	2.92	2.43	3.08	3.10	2.94	1.92	1.95	1.31
revPBE	1.64	1.65	2.33	2.34	2.90	2.92	2.43	3.09	3.11	2.95	1.92	1.95	1.31
mPBE	1.72	1.72	2.41	2.42	2.97	3.00	2.52	3.18	3.20	3.05	2.00	2.02	1.38
BOP	1.46	1.46	2.15	2.16	2.73	2.76	2.28	2.95	2.97	2.84	1.76	1.78	1.11
OPBE	1.62	1.62	2.30	2.30	2.91	2.93	2.41	3.09	3.11	2.94	1.89	1.92	1.30
OPerdew	1.74	1.74	2.42	2.43	3.03	3.05	2.54	3.21	3.23	3.07	2.02	2.04	1.43
OLYP	1.47	1.48	2.16	2.17	2.74	2.77	2.28	2.95	2.97	2.83	1.76	1.79	1.15
HCTH/407	1.82	1.83	2.51	2.53	3.10	3.13	2.65	3.33	3.34	3.22	2.11	2.14	1.49
Becke00	1.59	1.61	2.30	2.32	3.09	3.12	2.47	3.22	3.27	3.05	1.91	1.90	1.26
τ-HCTH	1.73	1.74	2.41	2.43	2.99	3.01	2.52	3.18	3.20	3.03	1.99	2.01	1.41
exptl[b]	1.87 ± 0.03		2.07 ± 0.03		2.59 ± 0.11		2.15 ± 0.15	3.21 ± 0.03			2.15 ± 0.15		1.51 ± 0.01

[a] Here Cl is a axial ligand. [b] Reference 23.

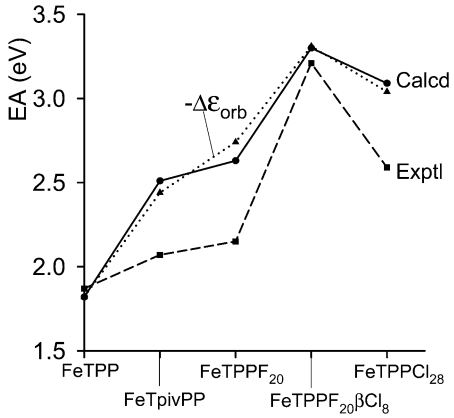

Figure 3. Schematic illustration of the calculated and experimental electron affinities (EAs). $\Delta\epsilon_{orbital}$ represents the difference of the $1e_g$ orbital energies between FeTPP and a substituted iron porphyrin.

calculated and experimental EAs, together with the difference of the $1e_g$ orbital energies ($-\Delta\epsilon_{orbital}$) between FeTPP and a substituted iron porphyrin. Here the orbital energy of FeTPP is set equal to the calculated EA of this system. We see that the calculated EAs are in excellent agreement with the $-\Delta\epsilon_{orbital}$ values. On the basis of the trend shown in the figure, the accuracy of the experimental EAs for FeTpivPP, $FeTPPF_{20}$, and $FeTPPCl_{28}$ appears to be questionable.

4. Conclusions

Compared to FeTPP, there is a significant Fe−N bond expansion in FeOTBP, $FeTPPCl_{28}$, and $FeTPPF_{20}\beta Cl_8$, accompanied by a significant decrease in the relative energy of the high-spin state. Therefore, the ground states of the latter three systems are all predicted to be high spin, where the energy ordering is reversed between the $^3A_{2g}$ and $^5A_{1g}$ states. The calculated result for FeOTBP is in agreement with the early experimental measurement, thereby changing the previous conclusion drawn from the calculations with only the BP functional. In these high-spin state complexes, no out-of-plane displacement of Fe is found.

In FeTpivPP, the relative energy of $^5A_{1g}$ decreases by ca. 0.05 eV as compared to that in FeTPP; the "picket fence" substituents at the *meso*-phenyl periphery are not found to cause an obvious decrease in the high-spin state's relative energy. The reliable calculations with the hybrid-GGA functionals still give an intermediate-spin ground state for FeTpivPP and they favor the $^3A_{2g}$ state over $^5A_{1g}$ by 0.05−0.15 eV. This seems to be at variance with the assignment of a high-spin state for this complex.[10]

The relative energy of the high-spin state in FeOEP is notably smaller than that in FeTPP. The calculated results with the hybrid-GGA functionals show the ground state to be either $^3A_{2g}$ or $^5A_{1g}$; their energies are too close to distinguish. This complex might exist as an admixed-spin ($S = 1, 2$) state.

It should be pointed out that the calculated ground states for $FeTPPCl_{28}$ and $FeTPPF_{20}\beta Cl_8$ are subject to verification through experimental studies. On the other hand, more detailed experimental investigations are desirable which might help to resolve the question of the FeTpivPP and FeOEP electronic structure. In this respect, the most useful experimental method would be an X-ray structural characterization that is able to provide the most convincing evidence as to whether the compound is intermediate or high spin because for iron porphyrins, there is an apparent correlation between the Fe−N bond length and the spin state of the iron ion (see Tables 2 and 3). Sometimes, the observed electromagnetic properties such as magnetic moment and Mössbauer resonance might not give a direct indication of the nature of the ground state.

Finally, the experimental results for the electron affinities (EAs) of FeTpivPP, $FeTPPF_{20}$, and $FeTPPCl_{28}$ may need to be refined; they appear to be too small by 0.4−0.5 eV based on our calculated trends in the EAs and in the orbital energies.

Acknowledgment. This work was supported by the National Science Foundation (NSF) CREST (grant HRD0318519), and by the NSF-EPSCoR (grant NSF 440900-362427-02). The ADF calculations were run on a QuantumCube QS4-2800C computer from Parallel Quantum Solutions (PQS), LLC.

Supporting Information Available: Optimized equatorial Fe−N bond lengths for selected states of FeTPP and FeOTBP with different density functionals (Table S1), comparison between the Non-SCF and SCF calculated relative energies for selected states of FeTPP and FeOTBP with the PBE, OPBE, or OLYP functional (Table S2), calculated relative energies and Fe−N bond lengths for selected states of FeTPP in D_{4h} and D_{2h} symmetry (Table S3), and Orbital energy level diagrams of FeTPP in the $^3E_g(A)$ (D_{4h}) and $^3B_{2g}$ (D_{2h}) states (Figure S1**)**. This material is available free of charge via the Internet at http://pubs.acs.org.

References and Notes

(1) *Iron Porphyrins*; Lever, A. B. P., Gray, H. B., Eds.; Addison-Wesley Publishing Company Inc.: Reading, MA, 1983.

(2) Collman, J. P.; Hoard, J. L.; Kim, N.; Lang, G.; Reed, C. A. *J. Am. Chem. Soc.* **1975**, *97*, 2676.
(3) Lang, G.; Spartalian, K.; Reed, C. A.; Collman, J. P. *J. Chem. Phys.* **1978**, *69*, 5424.
(4) Boyd, P. D. W.; Buckingham, A. D.; McMecking, R. F.; Mitra, S. *Inorg. Chem.* **1979**, *18*, 3585.
(5) Goff, H.; La Mar, G. N.; Reed, C. A. *J. Am. Chem. Soc.* **1977**, *99*, 3641.
(6) Mispelter, J.; Momenteau, M.; Lhoste, J. M. *J. Chem. Phys.* **1980**, *72*, 1003.
(7) Kitagawa, T.; Teraoka, J. *Chem. Phys. Lett.* **1979**, *63*, 443.
(8) Sontum, S. F.; Case, D. A.; Karplus, M. *J. Chem. Phys.* **1983**, *79*, 2881.
(9) Collman, J. P. *Inorg. Chem.* **1997**, *36*, 5145.
(10) Collman, J. P.; Gagne, R. R.; Reed, C. A.; Halbert, T. R.; Lang, G.; Robinson, W. T. *J. Am. Chem. Soc.* **1975**, *97*, 1427.
(11) (a) Collman, J. P.; Gagne, R. R.; Halbert, T. R.; Marchon, J.-C.; Reed, C. A. *J. Am. Chem. Soc.* **1973**, *95*, 7868. (b) Collman, J. P.; Gagne, R. R.; Reed, C. A. *J. Am. Chem. Soc.* **1974**, *96*, 2629.
(12) Sams, J. R.; Tsik, T. B. *Chem. Phys. Lett.* **1974**, *25*, 599.
(13) Kashiwagi, H.; Obara, S. *Int. J. Quantum Chem.* **1981**, *20*,dddddd 843.
(14) Dedieu, A.; Rohmer, M.-M.; Veillard, A. *Adv. Quantum Chem.* **1982**, *16*, 43.
(15) Rawlings, D. C.; Gouterman, M.; Davidson, E. R.; Feller, D. *Int. J. Quantum Chem.* **1985**, *28*, 773.
(16) Reiher, M.; Salomon, O.; Hess, A. *Theor. Chem. Acc.* **2001**, *107*, 48.
(17) Choe, Y.-K.; Nakajima, T.; Hirao, K. *J. Chem. Phys.* **1999**, *111*, 3837.
(18) Pierloot, K. *Mol. Phys.* **2003**, *101*, 2083.
(19) Kozlowski, P. M.; Spiro, T. G.; Bérces, A.; Zgierski, Z. *J. Phys. Chem. B* **1998**, *102*, 2603.
(20) Liao, M.-S.; Watts, J. D.; Huang, M.-J. *J. Comput. Chem.* **2006**, *27*, 1577.
(21) Liao, M.-S.; Scheiner, S. *J. Chem. Phys.* **2002**, *116*, 3635.
(22) Rovira, C.; Parrinello, M. *Chem. Eur. J.* **1999**, *5*, 250.
(23) Chen, H. L.; Ellis, P. E.; Wijesekera, T.; Hagan, T. E.; Groh, S. E.; Lyons, J. E.; Ridge, D. P. *J. Am. Chem. Soc.* **1994**, *116*, 1086.
(24) Liao, M.-S.; Watts, J. D.; Huang, M.-J. *J. Phys. Chem. A* **2005**, *109*, 11996.
(25) Hoard, J. L.; Hamor, M. J.; Hamor, T. A.; Caughey, W. S. *J. Am. Chem. Soc.* **1965**, *87*, 2312.
(26) Jentzen, W.; Turowska-Tyrk, I.; Scheidt, W. R.; Shelnutt, J. A. *Inorg. Chem.* **1996**, *35*, 3559.
(27) Byrn, M. P.; Curtis, C. J.; Hsiou, Y.; Khan, S. I.; Sawin, P. A.; Tendick, S. K.; Terzis, A.; Strouse, C. E. *J. Am. Chem. Soc.* **1993**, *115*, 9480.
(28) Maclean, A. L.; Foran, G. J.; Kennedy, B. J.; Turner, P.; Hambley, T. W. *Aust. J. Chem.* **1996**, *49*, 1273.
(29) Silvers, S. J.; Tulinsky, T. *J. Am. Chem. Soc.* **1967**, *89*, 3331.
(30) Brennan, T. D.; Scheidt, W. R.; Shelnutt, J. A. *J. Am. Chem. Soc.* **1988**, *110*, 3919.
(31) Cullen, D. L.; Meyer, J. E. F. *J. Am. Chem. Soc.* **1974**, *96*, 2095.
(32) Alden, R. G.; Crawford, B. A.; Doolen, R.; Ondrias, M. R.; Shelnutt, J. A. *J. Am. Chem. Soc.* **1989**, *111*, 2070.
(33) Czernuszewicz, R. S.; Li, X.-Y.; Spiro, T. G. *J. Am. Chem. Soc.* **1989**, *111*, 7024.
(34) Jentzen, W.; Unger, E.; Karvounis, G.; Shelnutt, J. A.; Dreybrodt, W.; Schweitzer-Stenner, R. *J. Phys. Chem.* **1996**, *100*, 14184.
(35) Jentzen, W.; Unger, E.; Song, X.-Z.; Jia, S.-L.; Turowska-Tyrk, I.; Schweitzer-Stenner, R.; Dreybrodt, W.; Scheidt, W. R.; Shelnutt, J. A. *J. Phys. Chem. A* **1997**, *101*, 5789.
(36) Rush, T. S.; Kozlowski, P. M.; Piffat, C. A.; Kumble, R.; Zgierski, M. Z.; Spiro, T. G. *J. Phys. Chem. B* **2000**, *104*, 5020.
(37) Piet, D. P.; Danovich, D.; Zuilhof, H.; Sudhölter, E. J. R. *J. Chem. Soc., Perkin Trans. 2* **1999**, 1653.
(38) Tsai, H.-H.; Simpson, M. C. *J. Phys. Chem. A* **2004**, *108*, 1224.
(39) Stoll, L. K.; Zgierski, M. Z.; Kozlowski, P. M. *J. Phys. Chem. A* **2002**, *106*, 170.
(40) Smirnov, V. V.; Woller, E. K.; DiMagno, S. G. *Inorg. Chem.* **1998**, *37*, 4971.
(41) Baerends, E. J.; Ellis, D. E.; Roos, P. *Chem. Phys.* **1973**, *2*, 41.
(42) te Velde, G.; Bickelhaupt, F. M.; van Gisbergen, S. J. A.; Fonseca-Guerra, C.; Baerends, E. J.; Snijders, J. G.; Ziegler, T. *J. Comput. Chem.* **2001**, *22*, 931.
(43) Fonseca-Guerra, C.; Snijders, J. G.; Baerends, E. J.; te Velde, G. *Theor. Chem. Acc.* **1998**, *99*, 391.
(44) *ADF2005.01*; SCM: Theoretical Chemistry, Vrije Universiteit, Amsterdam, The Netherlands, http://www.scm.com.
(45) Becke, A. D. *Phys. Rev. A* **1988**, *38*, 3098.
(46) Perdew, J. P. *Phys. Rev. B* **1986**, *33*, 8822.
(47) Perdew, J. P.; Burke, K.; Ernzerhof, M. *Phys. Rev. Lett.* **1996**, *77*, 3865.
(48) Zhang, Y.-K.; Yang, W.-T. *Phys. Rev. Lett.* **1998**, *80*, 890.
(49) Hammer, B.; Hansen, L. B.; Nørskov, J. K. *Phys. Rev. B* **1999**, *59*, 7413.
(50) Adamo, C.; Barone, V. *J. Chem. Phys.* **2002**, *116*, 5933.
(51) Tsuneda, T.; Suzumura, T.; Hirao, K. *J. Chem. Phys.* **1999**, *110*, 10664.
(52) Handy, N. C.; Cohen, A. J. *Mol. Phys.* **2001**, *99*, 403.
(53) Lee, C.; Yang, W.-T.; Parr, R. G. *Phys. Rev. B* **1988**, *37*, 785.
(54) Hamprecht, F. A.; Cohen, A. J.; Tozer, D. J.; Handy, N. C. *J. Chem. Phys.* **1998**, *109*, 6264.
(55) Boese, A. D.; Handy, N. C. *J. Chem. Phys.* **2001**, *114*, 5497.
(56) Becke, A. D. *J. Chem. Phys.* **2000**, *112*, 4020.
(57) Boese, A. D.; Handy, N. C. *J. Chem. Phys.* **2002**, *116*, 9559.
(58) Becke, A. D. *J. Chem. Phys.* **1993**, *98*, 5648.
(59) Becke, A. D. *J. Chem. Phys.* **1997**, *107*, 8554.
(60) Groenhof, A. R.; Swart, M.; Ehlers, A. W.; Lammertsma, K. *J. Phys. Chem. A* **2005**, *109*, 3411.
(61) Swart, M.; Groenhof, A. R.; Ehlers, A. W.; Lammertsma, K. *J. Phys. Chem. A* **2004**, *108*, 5479.
(62) Ghosh, A.; Vangberg, T.; Gonzalez, E.; Taylor, P. *J. Porphyrins Phthalocyanines* **2001**, *5*, 345.
(63) Ziegler, T.; Tschinke, V.; Baerends, E. J.; Snijders, J. G.; Ravenek, W. *J. Phys. Chem.* **1989**, *93*, 3050.
(64) Dolphin, D.; Sams, J. R.; Tsin, T. B.; Wong, K. L. *J. Am. Chem. Soc.* **1976**, *98*, 6970.